

**Photodesorption of oxygen from carbon nanotubes**

Yoshiyuki Miyamoto

*Fundamental Research Laboratories, NEC Corporation, 34 Miyukigaoka, Tsukuba, 305-8501, Japan*

Noboru Jinbo\* and Hisashi Nakamura

*Research Organization for Information Science & Technology (RIST), 2-2-54, Nakameguro, Meguro, Tokyo, 153-0061, Japan*

Angel Rubio

*Departamento Fisica de Materiales, Facultad de Quimicas, Universidad del País Vasco, Centro Mixto CSIC-UPV/EHU and Donostia International Physics Center (DIPC), Apartado 1072, 20018 San Sebastian/Donostia, Spain*

David Tománek

*Department of Physics and Astronomy, Michigan State University, East Lansing, Michigan 48824-2320, USA*

(Received 11 October 2004; published 28 December 2004)

We propose to use photodesorption as a noninvasive tool to clean carbon nanotubes from oxygen, offering a clear advantage over thermal and chemical treatments. The detachment of chemisorbed oxygen from atomic vacancies is triggered by a resonant Auger process, initiated by an  $O\ 1s \rightarrow O\ 2p$  transition, which leaves two holes in the  $O\ 2s$  level. In the electronically excited state, oxygen desorbs spontaneously, with no damage to the carbon network or the cylindrical nanotube shape. Subsequent reaction of oxygen atoms with  $H_2$  molecules is shown to prevent reoxidation of the nanotube.

DOI: 10.1103/PhysRevB.70.233408

PACS number(s): 81.07.De, 61.48.+c

Oxidation is commonly used to purify carbon nanotubes (CNTs) from amorphous carbon soot.<sup>1</sup> The efficiency of this process relies on the fact that carbon soot converts easily to CO and CO<sub>2</sub>, which subsequently evaporate, in contrast to structurally perfect nanotubes and graphite, which are rather unreactive. *Ab initio* density functional theory (DFT) calculations<sup>2,3</sup> indeed suggest that the interaction of molecular oxygen with carbon nanotubes should be weak, in stark contrast to the dissociative adsorption of oxygen atoms at the edges<sup>4</sup> and at defect sites<sup>5</sup> of carbon nanotubes. There, chemisorbed oxygen forms chemically strong C—O—C complexes, which have been observed by near-edge x-ray absorption fine-structure spectroscopy.<sup>6</sup> Whereas physisorption of O<sub>2</sub> causes hole doping and increases the electronic conductivity of semiconductor nanotubes,<sup>2</sup> formation of C—O—C complexes destroys the perfect  $\pi$ -bonding network and thus decreases the conductivity of nanotubes. Finding an effective way to remove the chemisorbed oxygen is a necessary prerequisite for a practical use of carbon nanotubes in electronic devices.

Removal of the chemisorbed oxygen atoms by heat treatment comes with the inevitable side effect of damaging the carbon network surrounding the O atom, due to the higher stability of the C—O bond in comparison to C—C bonds.<sup>4</sup> Such structural damage is evidenced in temperature programmed mass spectra of oxidized carbon nanohorns,<sup>7</sup> with a graphitic network similar to nanotubes, which show a preferential desorption of CO and CO<sub>2</sub> molecules rather than oxygen at high temperatures. The stability of the C—O bond also makes alternative chemical processes, designed for selectively breaking the C—O bond, very unlikely. The inertness of the C—O—C complex in a defective nanotube was confirmed by our DFT calculations, which suggest that H atoms preferentially attach to carbon rather than oxygen sites. Inspired by the observed disintegration of H<sub>2</sub>O mol-

ecules by a resonant Auger process,<sup>8</sup> we decided to study photochemical processes in oxidized nanotubes as an alternative to chemical and thermal purification methods.

Here we propose to use photodesorption as an efficient, noninvasive way to clean carbon nanotubes from chemisorbed oxygen. Results of our first-principles simulations for electron ion dynamics (FPSEID)<sup>9</sup> suggest that the strong C—O bonds can be efficiently ruptured by optically promoting the bonding electrons into an excited state by a resonant Auger process. This initiates a desorption of the oxygen atom with no damage to the surrounding carbon network.

Our study of the photodesorption process is based on *ab initio* molecular dynamics (MD) simulations on the adiabatic potential energy surface (APES) associated with an electronically excited state. To correctly follow the APES we have combined time-dependent DFT (TDDFT) (Ref. 10) with classical Newton's equations of motion for the ions in FPSEID.<sup>9</sup> This type of computational approach turns out to be particularly challenging because the study precludes the solution of the time-dependent Schrödinger equation for the time evolution of the electronic wave functions in the presence of ionic motion, caused by the changing charge distribution. So far we have implemented this scheme in computer codes FPSEID (Ref. 9) and OCTOPUS.<sup>11</sup> FPSEID cares about numerical stability in the simulation of the order of 100 fs, but with needs of huge core-memory and longer computation time. This scheme is valid unless the system significantly deviates from the APES due to a nonradiative decay of the excited state. The main benefit of the TDDFT approach is its ability to correctly populate the electronic states even in case of level alternation. We use the local density approximation<sup>12</sup> (LDA) to DFT and confirmed the validity of our photodesorption results by using the alternative generalized gradient approximation<sup>13,14</sup> (GGA) for the exchange-correlation functional. We described the interaction between valence elec-

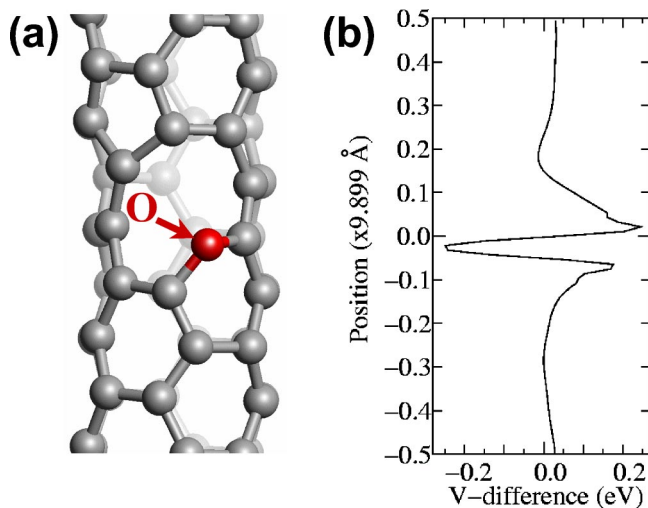


FIG. 1. (Color online) (a) Structure of the C—O—C complex in a defective C(3,3) nanotube. (b) Difference between the self-consistent LDA potential  $V$  of the structure in (a), containing the C—O—C complex, and a reference structure with no oxygen, but all carbons in the same positions.  $V$ -difference is averaged in the plane normal to the tube axis and does not contain contributions from the nonlocal part of the pseudopotentials. The same vertical length scale is used in (a) and (b).

trons and ions by separable norm-conserving pseudopotentials<sup>15</sup> and used a plane-wave basis with a cutoff energy of 60 Ry in all the calculations.

We have focused on the C(3,3) armchair nanotube, one of the thinnest nanotubes synthesized to date.<sup>16</sup> We have imposed three-dimensional periodic boundary conditions, effectively describing a nanotube bundle with triangular packing and an interwall distance of 4 Å. To minimize coupling between defect sites, we used four primitive unit cells of the pristine (3,3) nanotube as a unit cell in the axial direction, as shown in Fig. 1(a), and used the  $\Gamma$  point to sample the one-

dimensional Brillouin zone.

The starting point of all APES simulations of the photoexcitation process, described in the following, was the equilibrated structure of the oxidized nanotube in the electronic ground state, depicted in Fig. 1(a). The formation of a pentagon opposite the oxygen adsorption site was found energetically favorable due to the saturation of dangling bonds. The effect of the oxygen atom on the self-consistent potential of the defective tube is demonstrated in Fig. 1(b). The presence of the O atom causes a sharp dip in the potential, which leads to a strong scattering and trapping of carriers near the C—O—C complex, thus decreasing the nanotube conductance as mentioned before.

In order to investigate the possibility of photodesorbing the oxygen atom, we considered a sudden electronic excitation from the localized O  $2s$  orbital in the frozen ground-state geometry. The electronic spectrum of this system is shown in Fig. 2(a). We find the O  $2s$  level to lie well below the nanotube valence band. The O  $2p$  state, on the other hand, hybridizes strongly with O  $2p$  states, forming a bonding and an antibonding state. Close inspection of the oxygen-related states, represented in the insets in Fig. 2(a), suggests that the O  $2s$  state has a bonding character and hybridizes only moderately with the  $2p$  orbitals of the neighboring C atoms. The O  $2p$ —C  $2p$  hybrid state, which lies in resonance with the nanotube conduction band, shows an antibonding character.<sup>17</sup> Consequently, we would expect the O  $2s \rightarrow$  O  $2p$  excitation, requiring a vertical excitation energy of 33 eV,<sup>18</sup> to weaken the C—O bond and to cause a possible desorption of the oxygen atom.

The structure evolution during this photoexcitation process, as obtained by the FPSEID simulation, is shown by several snapshots in Fig. 2(b). Our results indicate that following the O  $2s \rightarrow$  O  $2p$  photoexcitation, the C—O bond length extends significantly from 1.40 to 1.90 Å. In spite of this large bond elongation, the C—O—C complex remains intact without any indication of O emission. We expect that such excitations should only heat up the nanotube, but

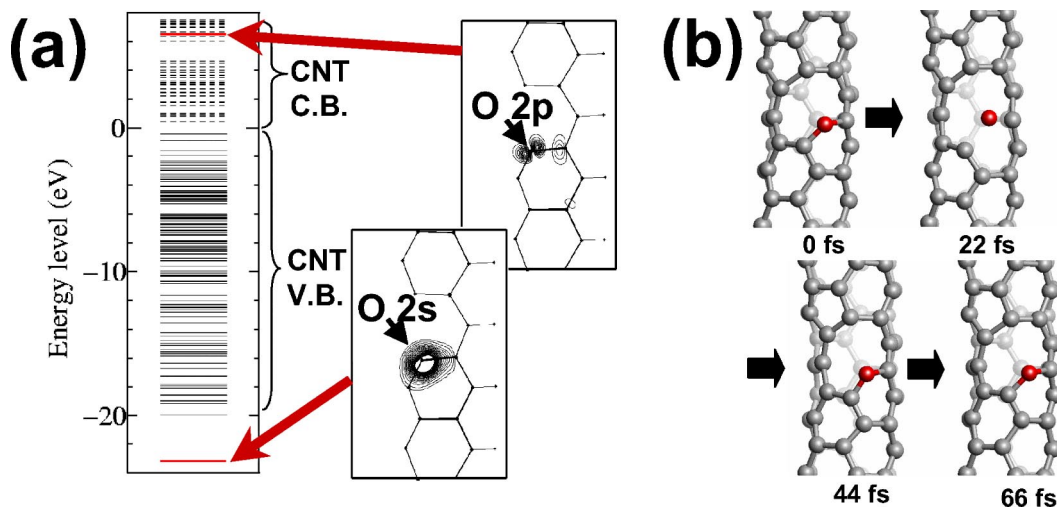


FIG. 2. (Color online) (a) Electronic structure of the system in Fig. 1(a). Valence states at the  $\Gamma$  point are shown by solid lines and conduction states by dashed lines. The insets show the charge density maps corresponding to the O  $2s$  level, lying below the nanotube valence band, and the O  $2p$  level, lying within the nanotube conduction band. (b) Time evolution of the C—O—C complex following an O  $2s \rightarrow$  O  $2p$  excitation.

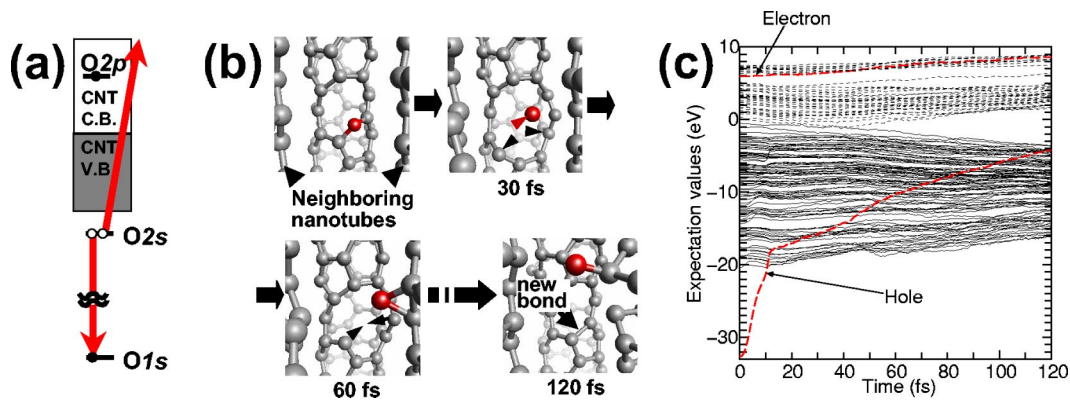


FIG. 3. (Color online) (a) Schematics of the resonant Auger decay following an initial  $O 1s \rightarrow O 2p$  excitation, with two holes in the  $O 2s$  and one extra electron in the  $O 2p$  level in the final state.<sup>19</sup> The arrows depict the relaxation of the  $O 1s$  hole followed by the emission of the  $O 2s$  electron. Also shown is the position of the relevant oxygen levels with respect to the valence band (VB) and the conduction band (CB) of the nanotube. (b) Snapshots of the MD simulation starting from the Auger state shown in (a). Arrows are used to guide the eye when following the atomic motion. (c) Time evolution of the expectation value of all single-particle states throughout the entire MD simulation. The heavy dashed lines denote the evolution of the initially excited electron (upper curve) and the two holes (lower curve). Conduction band states of the nanotube are shown by the dotted lines.

should not trigger a desorption of the chemisorbed oxygen.

As a viable alternative, we studied the resonant Auger process, initiated by exciting one  $O 1s$  core electron to the  $O 2p$  level, which requires an energy of  $\approx 530$  eV.<sup>6</sup> The subsequent Auger process of interest in the present context, depicted in Fig. 3(a),<sup>19</sup> leads to a final state with two holes in the  $O 2s$  level.<sup>20</sup> As we will show in the following, this final-state electronic configuration will cause a spontaneous emission of the O atom and a subsequent self-healing of the created vacancy due to the formation of a new C—C bond.

We assume that the Auger process spontaneously follows the  $O 1s \rightarrow O 2p$  photoexcitation and start the simulation in the Auger state shown in Fig. 3(a).<sup>19</sup> Figure 3(b) shows snapshots of the MD simulation of the oxidized C(3,3) nanotube, depicting the O emission from the C—O—C complex. Only 30 fs after the photoexcitation, we observe the initial escape of the O atom from the nanotube. Meanwhile, the two C neighbors are pushed back, initially enlarging the vacancy size. Another 30 fs later, these C atoms change their direction of motion and start approaching each other. Then, 120 fs after the photoexcitation, the two carbon atoms approach sufficiently to form a new bond, indicative of a self-healing mechanism, which had been postulated to occur in thin carbon nanotubes.<sup>21</sup>

The time evolution of the expectation values of all single-particle states throughout the MD simulation is shown in Fig. 3(c). Upon depopulation at  $t=0$ , the energy eigenvalue of the  $O 2s$  level drops by more than 10 eV with respect to its value in the ground state, shown in Fig. 2(a).<sup>22</sup> This drop is followed by its rapid rise into the nanotube valence band region during the first 10 fs. The observed alternation of the  $O 2s$  level with nanotube bands is generally expected to cause a nonadiabatic decay of the excitation. This decay does not occur in our simulation due to the weak overlap between the  $O 2s$  orbital and the nanotube valence states. Consequently, the excited state dynamics follow the corresponding adiabatic potential energy surface for an extended time period.

As shown in Fig. 3(b), the ejection of the O atom from the C—O—C complex occurs without any adverse effect on the carbon network. When occurring in a bundle, represented by the boundary conditions in our simulation, the ejected O atom may readsorb at a neighboring tube. This process indeed occurs 120 fs after the photoexcitation, as seen in Fig. 3(b). To help prevent the oxygen from readsorbing on a nanotube, we consider ways to render oxygen less reactive. A viable scenario would be to expose the oxidized nanotube to an  $H_2$  atmosphere, with the hope of forming  $H_2O$  molecules following the deoxidation process.

The results of our corresponding simulation with one  $H_2$  molecule per unit cell are shown as a series of snapshots in Fig. 4. We find that the spontaneous photodesorption of the oxygen atom in the Auger state shown in Fig. 3(a) (Ref. 19) proceeds similar to the process depicted in Fig. 3(b). Rather than readsorbing on a nanotube, the O atom reacts with  $H_2$  and forms an  $OH^+$  radical. We expect this  $OH^+$  radical to eventually neutralize and react with the lone H atom to form a water molecule, but did not observe this reaction in the limited time period of our simulation. In spite of the uncertainty about the final state of the desorbed oxygen, our results strongly indicate that exposing the oxidized nanotube to an H atmosphere during the resonant Auger process is an efficient way to deoxidize nanotubes and prevent their reoxidation.<sup>14</sup>

The main benefit of the state with a completely depopulated  $O 2s$  level is its long lifetime, which we found to be crucial for the O emission. The long lifetime, depicted in Fig. 3(c), is caused by the spatial separation between the  $O 2s$  orbital and the nanotube valence wave functions. Similar long lifetimes in the order of  $10^{-13}$  s of  $O 2s$  holes were also reported during the reactions of ionized O atoms with Pt(111) (Ref. 23) and TiC(111) (Ref. 24) surfaces, and should remain a common feature also in other carbon nanotubes.

As an alternative to the Auger state depicted in Fig. 3(a),<sup>19</sup> one may consider the system dynamics starting from an Auger final state with only one hole in the  $O 2s$  level and no

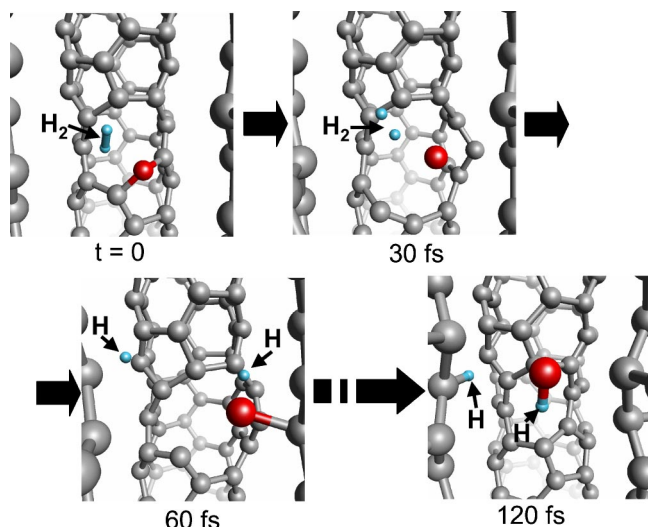


FIG. 4. (Color online) Dynamics of the C—O—C complex in the presence of a  $H_2$  molecule, starting from the same Auger final state as considered in Fig. 3.

extra electron populating the  $O\ 2p$  level. We do not believe that oxygen desorption should be enhanced in this state because a partial population of the  $O\ 2s$  level should stabilize the C—O bond, and the depopulation of the nonbonding  $O\ 2p$  state should have little effect on the stability of the C—O—C complex.

In summary, we have proposed to use photodissociation as an efficient tool to clean carbon nanotubes from chemisorbed oxygen. We have shown that spontaneous detachment of chemisorbed oxygen is triggered by a resonant Auger process, initiated by the  $O\ 1s \rightarrow O\ 2p$  excitation, which leaves two holes in the  $O\ 2s$  state. Our results, obtained for a 4 Å wide nanotube, are expected to hold also for other nanotubes. The vacancy formed by the oxygen emission may heal spontaneously, as a new C—C bond is formed, which helps the nanotube maintain its structural integrity and shape. Readorption of oxygen may be prevented by a secondary reaction between oxygen and hydrogen molecules, yielding water. Due to its noninvasiveness and precision, “photosurgical” deoxidation should offer a clear advantage over thermal and chemical treatments.

The FPSEID simulations were performed on the SX-5 vector-parallel system at the NEC Fuchu Plant and on the Earth Simulator supercomputer in Yokohama. Y.M. is indebted to T. Kawai, T. Kurimoto, and T. Noguchi for parallelizing the FPSEID computer code. Y.M. and D.T. acknowledge support by the Computational Nano-Technology (CNT) program managed by M. Endo. A.R. acknowledges support from the European Community 6th framework Network of Excellence NANOQUANTA (NMP4-CT-2004-500198) Spanish MCyT and the University of the Basque Country. D.T. was partly supported by the NSF-NIRT Grant No. DMR-0103587.

\*Present address: Advanced Systems Design and Engineering Dept., Isogo Nuclear Engineering Center, Toshiba Corp., 8 Shin-Sugita Cho, Isogo-Ku, Yokohama, 253-8523, Japan.

<sup>1</sup>See, for example, S. Gajewski *et al.*, *Diamond Relat. Mater.* **12**, 816 (2003).

<sup>2</sup>S. H. Jhi *et al.*, *Phys. Rev. Lett.* **85**, 1710 (2000).

<sup>3</sup>P. Giannozzi *et al.*, *J. Chem. Phys.* **118**, 1003 (2003).

<sup>4</sup>S. M. Lee *et al.*, *Phys. Rev. Lett.* **85**, 2757 (2000).

<sup>5</sup>M. S. C. Mazzoni *et al.*, *Phys. Rev. B* **60**, R2208 (1999).

<sup>6</sup>A. Kuznetsova *et al.*, *J. Am. Chem. Soc.* **123**, 10699 (2001).

<sup>7</sup>E. Bekyarova *et al.*, *Chem. Phys. Lett.* **366**, 463 (2002).

<sup>8</sup>M. Nagasono *et al.*, *Chem. Phys. Lett.* **298**, 141 (1998).

<sup>9</sup>O. Sugino and Y. Miyamoto, *Phys. Rev. B* **59**, 2579 (1999); **66**, 089901 (2002).

<sup>10</sup>E. Runge and E. K. U. Gross, *Phys. Rev. Lett.* **52**, 997 (1984).

<sup>11</sup>M. A. L. Marques *et al.*, *Comput. Phys. Commun.* **151/1**, 60 (2003).

<sup>12</sup>J. P. Perdew and A. Zunger, *Phys. Rev. B* **23**, 5048 (1981); D. M. Ceperley and B. J. Alder, *Phys. Rev. Lett.* **45**, 566 (1980).

<sup>13</sup>J. P. Perdew and Y. Wang, *Phys. Rev. B* **45**, 13244 (1992).

<sup>14</sup>We have found our results not to depend strongly on the exchange-correlation functional used in DFT. The forces acting on the oxygen atom in the Auger final state, obtained using GGA, were generally stronger than LDA-based forces. Consequently, the predicted photo-induced oxygen desorption is activation-free both in GGA and LDA and should occur even faster in a GGA than in our LDA simulation.

<sup>15</sup>N. Troullier and J. L. Martins, *Phys. Rev. B* **43**, 1993 (1991); L.

Kleinman and D. M. Bylander, *Phys. Rev. Lett.* **48**, 1425 (1982).

<sup>16</sup>L.-C. Qin *et al.*, *Nature (London)* **408**, 50 (2000); N. Wang *et al.*, *ibid.* **408**, 50 (2000); T. Hayashi *et al.*, *Nano Lett.* **3**, 887 (2003).

<sup>17</sup>This character analysis is based on calculated overlaps with the wave functions of an oxygen pseudoatom.<sup>15</sup>

<sup>18</sup>The calculated excitation energy of 33 eV is based on the total energy difference between the ground and the excited states within LDA.

<sup>19</sup>In our simplified description, we exclude the four valence electrons in the  $O\ 2p$  level from the discussion because they are not affected by the Auger process.

<sup>20</sup>To treat adequately the  $+1e$  net charge per unit cell in the Auger final state, we superposed a uniform negative background charge to keep the system charge neutral. The negative background charge was treated separately from the real charges in the system to avoid fictitious Coulomb interactions, which may otherwise cause artifacts in systems with periodic boundary conditions.

<sup>21</sup>S. Berber *et al.*, *Physica B* **323**, 78 (2003).

<sup>22</sup>The substantial drop in the  $O\ 2s$  orbital energy following its depopulation in the O-CNT system can be compared to the behavior of an isolated atom. There, both LDA and GGA suggest a similar  $O\ 2s$  orbital lowering after a neutral oxygen atom with the electronic configuration  $O\ 1s^2 2s^2 2p^4$  has acquired a single positive charge in the  $O\ 1s^2 2s^0 2p^5$  state.

<sup>23</sup>R. Souda *et al.*, *Phys. Rev. B* **51**, 4463 (1995).

<sup>24</sup>R. Souda *et al.*, *J. Chem. Phys.* **112**, 979 (2000).